Short Communication

Synthesis of Porous Carbon Sphere Based on Starch and Its Application of Electric Double Layer Capacitor

Bo Zhou[1,2], Erlin Meng[1], Zhenqian Chen[2,]*

[1] SUST, School of Environment Science and Engineering, Suzhou University of Science and Technology, Suzhou, 215009, P. R. China
[2] IIUSE, Key Laboratory of Energy Thermal Conversion and Control of Ministry of Education, School of Energy and Environment, Southeast University, Nanjing, 210096, P. R. China
[*]E-mail: zhenqiancheniiuse@163.com

The present work reported the preparation of mesoporous activated carbon spheres (MCS) based on potato starch through the activation of CO_2. N_2 adsorption strategy was employed to investigate the influences of activation time and temperature on the MCS properties. On the other hand, the galvanostatic charge–discharge and cyclic voltammetry (CV) were applied to analyze the influence of the porosity on its electrochemical behaviors. The electrochemical experiment results confirmed that MCS was distinctive in its capacitive property and only has slight internal resistance. This corresponded to the maximal specific capacitance value.

Keywords: Double layer capacitor; Carbon sphere; Graphene; Starch; Cyclic voltammetry

1. INTRODUCTION

Electrochemical supercapacitors, high-rate energy storage and delivery tools, have many different commercial applications, including hybrid electric vehicles, memory back-up systems, energy efficient industrial equipments, and consumer electronics [1-4]. Compared with traditional batteries/capacitors, these supercapacitors are more favorable, considering their distinctive advantages, such as low maintenance, long cycle life, high charging-discharging rate, along with high energy density and power density [5-8]. Based on the energy-storage mechanism, supercapacitors fall into two categories: pseudocapacitors and electrical double-layer capacitors (EDLCs). Comparatively, the latter kind of supercapacitors has longer recycle life and higher energy efficiency, considering the absence of faradic reaction and remarkable electronic conductivity [9, 10]. EDLCs have been the main commercial supercapacitors until now. At the interface between electrolyte and electrode materials in

the case of EDLCs, an electrical double layer is formed to store electric energy [11, 12]. Therefore, the energy-storage capacity of electrode materials strongly depends on the their surface features such as surface chemistry and surface area.

Porous carbons are extensively for EDLCs as electrode materials, including graphene-based materials, carbon nanotubes (CNTs), ordered mesoporous carbons, regular microporous/ultramicroporous carbons, and activated carbons [13-16]. The pore structure and surface area of the porous carbon materials have significant effects on their capacitive behavior. In brief, the electrochemical capacities can be improved due to their large surface area providing sufficient regions for ions to accumulate [17-19]. However, for commercial activated carbon, many surface areas of micropores could not engage into the charge-storage process of EDLCs; on the other hand, the diffusion of electrolyte ions onto inner pore wall will be limited by many of its island and irregular micropores, which lead to a poor capacitive behavior of electrode materials [20, 21]. Furthermore, the transfer of electrolyte ions in electrodes can be accelerated due to the macroporous structure, while the macroporous carbons suffer limited surface area of electrode. In the case of mesoporous channels (pore size: 2–8 nm), the electrochemical behavior will be enhanced by both a quantity of inner surface area for charge storage, and accelerated kinetic process of electrolyte ion diffusion in the electrodes [22, 23]. Thus, many different techqniues have been reported for preparing carbonaceous materials with mesoporous structure, such as chemical activation approaches and template strategies [24-27].

The formation of MCS from renewable materials has gained increasingly more attention recently [27-29]. Potato starch, a vital carbon precursor, has certain granule shape and can be obtained from many different renewable plants. However, rare studies have been reported on the synthesis of MCS from starch. In the present work, the MCS are prepared based on potato starch through KOH activation, together with its electrochemical property investigation [30-32]. In general, chemical or physical strategy has been used to prepare activated carbon. Based on the same precursor, the prepared activated carbon may have different properties with different synthesis parameters and activation techniques.

In the present study, a highly porous MCS was developed based on photo starch. Our proposed MCS has a suitable pore size (~2.55 nm) as well as a large surface area (2437.1 m^2/g). In addition, the ion diffusion distance from bulk solution to active sites can be significantly shortened due to the porosity and nanosize of the spherical structure. It outperforms other materials prepared in the absence of $ZnCl_2$ when employed for supercapacitors as electrode materials in the electrolyte (2 M aqueous KOH solution) due to its distinctive capacitive features.

2. EXPERIMENTS

2.1. Preparation of MCS

Potato starch was obtained from Jiangsu Zhongliang Co., LTD. Initially the potato starch first stabilized at 180 °C in air atmosphere overnight. A tube furnace was used for activation. As the activation began, the N_2 was passed through the furnace. The temperature of this furnace was raised up

to 600 °C and kept for 1 hr. Afterwards the furnace temperature was further raised up to activation temperatures and kept for a given time. The gas medium was substituted by CO_2 (flow rate: 30 mL/min) upon reaching the activation temperature. After the activation process was ended, the gas medium was changed back into N_2, with the furnace left cooling to ambient temperature. The MCS after activation at 750 °C, 800 °C and 900 °C referred to MCS-1, MCS-2 and MCS-3, respectively.

2.2. Electrode preparation and electrochemical measurements

For the preparation of the two-electrode capacitors, the polypropylene membrane was used as a separator. The constituting components of the electrode are: MCS (85 wt%), acetylene black (10 wt%), and polytetrafluoroethylene (5 wt%). The test electrolyte was an aqueous solution of 6 M KOH. An Land CT2001A battery test instrument and CHI604A electrochemical geometry were used for the galvanostatic charge–discharge measurement and cyclic voltammetry (CV) experiment, respectively.

3. RESULTS AND DISCUSSION

This study investigated the influence of different factors on the surface area (S_{BET}), total volume (V_{total}) and yield of MCS. The former two factors of MCS increase as the activation temperature increase in a range of 750 and 900 °C. In addition, all samples show a low S_{BET}, which suggests the MCS with high surface areas could not be favorably prepared at low activation temperature. The yield is reduced to 64% at a high activation temperature of 900 °C, since the high temperature is in favor of the endothermic reaction between CO_2 and carbon [33]. Thus 900 °C is selected as the optional temperature to study the influence of activation time on MCS properties (Table 1). As the activation proceeds, a decrease in MCS yield can be found, since abundant micropores are formed. The formation occurs since the increasing number of carbon atoms at the active sites react with CO_2 as the activation proceeds. However, S_{micro} of sample only increases, which suggests the synchronous occurrence of the micropore formation, along with micropore widening and deepening; and the rate of formation is lower than that of the other two at prolonged activation time.

Table 1. Surface area and pore volume of MCS prepared by CO_2.

Sample	Yield(%)	S_{BET} (m^2/g)	S_{micro} (m^2/g)	V_{total}(cm^3/g)	V_{micro}(cm^3/g)
MCS-1	94	502	395	0.23	0.22
MCS-2	77	1387	1322	1.15	0.87
MCS-3	64	1433	1357	1.33	0.99

Fig. 1 shows the nitrogen adsorption/desorption isotherms of MCS, along with the corresponding pore size distribution curves. Comparable isotherms are observed for MCS samples. MACS-2 shows a sharply increased amount of adsorbed N_2 compared with MACS-1; then MACS-3 exhibits a gradually increased amount than MACS-2, which suggests their comparable porous

structures, as well as varied pore volumes and surface areas. At higher pressure region, the N_2 adsorption is sharply increased at these MACS samples, as shown in the isotherms. The may result from the curve combination of type I and IV isotherms that are indicative of the microporous-mesoporous porosity conversion. MCS have comparable pore structure, with a distribution centered at ~2.55 nm, with the MCS pore size mainly distributed in micropore region, as shown in the pore size distribution of Fig. 1B.
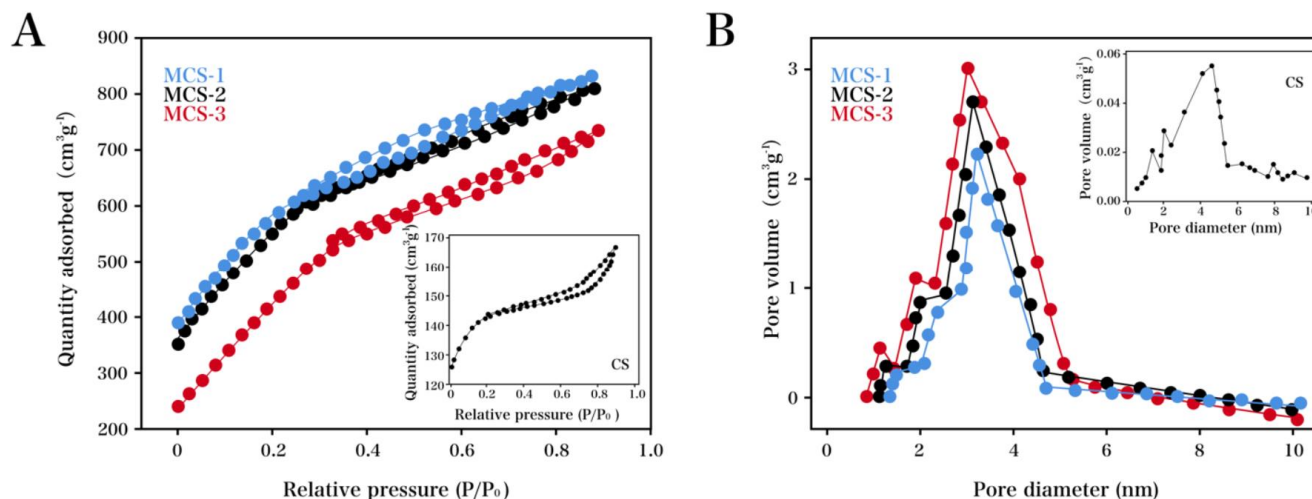
Figure 1. (A) Nitrogen adsorption/desorption isotherms recorded for MCS; (B) The pore size distribution curves of MCS.

Different electrochemical properties of normal CS and MCS synthesized under different activation temperature are shown in Fig. 2. For the MCS, a comparable rectangular shape can be observed, along with varied areas (corresponding to specific capacitance), as displayed in the CV profile in Fig. 2A. On the other hand, the specific capacitance values in CV were obtained through the equation as follows:

$$C = \int IdV / mVv$$

where I (A) and V (V) are the response current density and potential; v (mV/s) and m (g) are the potential scan rate and the electroactive material mass in the electrode. At CS, small rectangle can be observed, with a specific capacitance of 22.3 F/g. However, relatively large areas are recorded for the MCS, which is increased with enhanced activation. And MACS-1, MACS-2, and MACS-3 show the specific capacitances of 125.7, 152.9, and 161.9 F/g, respectively (scan rate: 50 mV/s). The above electrode materials are also characterized by galvanostatic charge/discharge curves (constant current: 1 A/g), as shown in Fig. 2B. At the same current density, MACS-3 electrode shows remarkably longer galvanostatic discharge time compared with the controls, which suggests a specific capacitance increase. This result agrees well with that from the CV experiments. The following equation presents the calculation of the MCS specific capacitances according to galvanostatic charge/discharge curves:

$$C = I\Delta t / m\Delta V$$

where I (A) and Δt (s) are the discharging current and discharging time. m (g) and ΔV (V) are the electrode material mass and discharging potential range. C (F/g) refers to the specific capacitance

of the electrode. For MACS-1, MACS-2, and MACS-3, the specific capacitances are 195.7, 182.3, and 156.7 F/g, respectively (constant current: 1 A/g), as shown in the discharge curves.
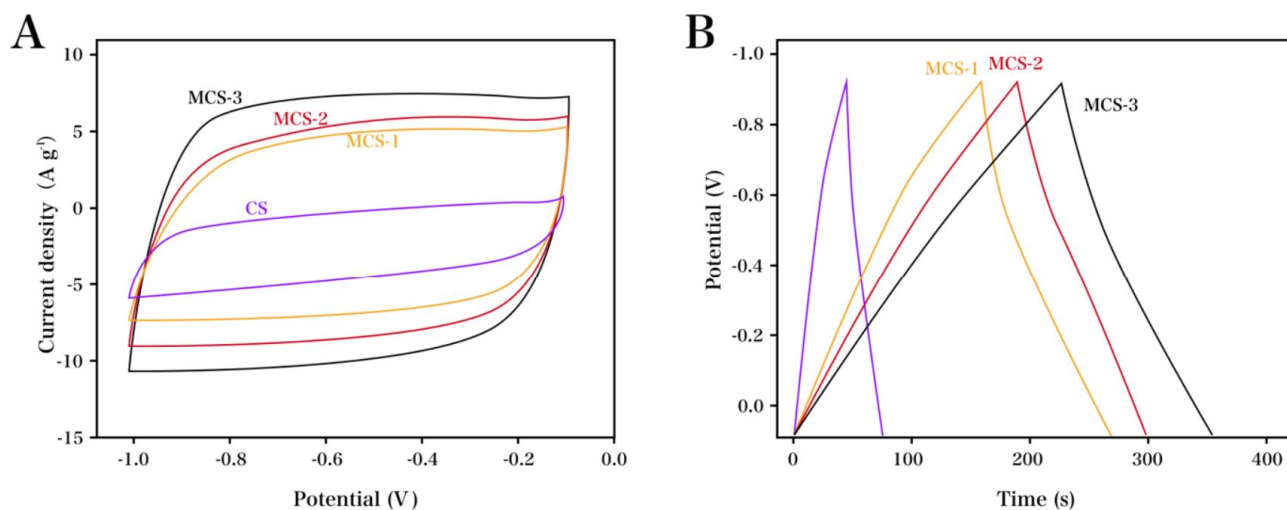

Figure 2. Different electrochemical features of MCS and CS: **(A)** CVs obtained at a sweep rate of 50 mV/s; **(B)** galvanostatic charge/discharge curves recorded at a current density of 1 A/g.

Fig. 2 displays the CVs of MCS-2 and MCS-3 at varying scan rates. The typical rectangular shape can be seen for the two samples when the scan rate is low at 10 mV/s, indicative of desirable capacitance performances. MCS-2 shows a larger CV curve area when the specific capacitance is increased, consistent with the results from the charge–discharge experiment. The MCS-2 displays a jujube-stone shaped CV curve at scan rate of 100 mV/s, whereas MCS-3 still shows a rectangular CV, due to the easier electrolyte ion transfer at MCS-3 with up to 43% high mesopore contents. This phenomenon suggests that the electrolyte ion transfer can also be accelerated by the mesopores, besides the storage of electric double layer. Thus, apart from the surface areas increase, another effective approach to enhancing the specific capacitance of electric double-layer capacitor (esp. at high charge–discharge rate) is to increase the mesopore proportion.
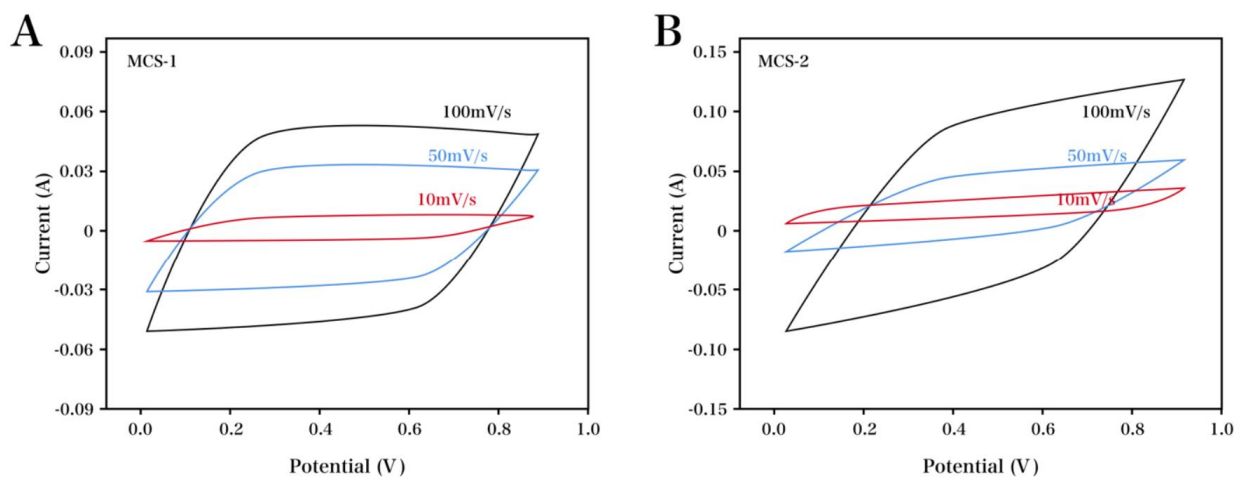

Figure 3. CV curves of MCS-2 and MCS-2 at different scan rates.

4. CONCLUSIONS

In the present study, the MCS was synthesized based on potato starch. And the BET strategy was used to study the effects of activation time and temperature. The results confirm that MCS can be applied to the application of the electric double layer capacitor its favorable pore structure.

References

1. E.M. Garcia, H.A. Tarôco, T. Matencio, R.Z. Domingues, J.A.F.D. Santos, R.V. Ferreira, E. Lorençon, D.Q. Lima and M.B.J.G.D. Freitas, *Journal of Applied Electrochemistry*, 42 (2012) 361.
2. Y.J. Lee, W.P. Hai, S. Park and I.K. Song, *Current Applied Physics*, 12 (2012) 233.
3. X. Ma, L. Gan, M. Liu, P.K. Tripathi, Y. Zhao, Z. Xu, D. Zhu and L. Chen, *Journal of Materials Chemistry A*, 2 (2014) 8407.
4. L. Ding, Z. Wang, Y. Li, Y. Du, H. Liu and Y. Guo, *Mater. Lett.*, 74 (2012) 111.
5. B.B. Sales, F. Liu, O. Schaetzle, C.J.N. Buisman and H.V.M. Hamelers, *Electrochimica Acta*, 86 (2012) 298.
6. L. Li, J. Qiu and S. Wang, *Electrochimica Acta*, 99 (2013) 278.
7. S. Giri, D. Ghosh and C.K. Das, *Journal of Electroanalytical Chemistry*, 697 (2013) 32.
8. S. Shivakumara, Z. Tirupathi, P. Rao and N. Munichandraiah, *Ecs Electrochemistry Letters*, 2 (2013) A60.
9. P. Li, Y. Yang, E. Shi, Q. Shen, Y. Shang, S. Wu, J. Wei, K. Wang, H. Zhu and Q. Yuan, *ACS applied materials & interfaces*, 6 (2014) 5228.
10. P.K. Nayak and N. Munichandraiah, *Journal of Solid State Electrochemistry*, 16 (2012) 2739.
11. W. Du, Z. Wang, Z. Zhu, S. Hu, X. Zhu, Y. Shi, H. Pang and X. Qian, *Journal of Materials Chemistry A*, 2 (2014) 9613.
12. S. Faraji and F.N. Ani, *Renewable & Sustainable Energy Reviews*, 42 (2015) 823.
13. X. Du, W. Zhao, Y. Wang, C. Wang, M. Chen, T. Qi, C. Hua and M. Ma, *Bioresource Technology*, 149 (2013) 31.
14. X. Sun, X. Zhang, H. Zhang, B. Huang and Y. Ma, *Journal of Solid State Electrochemistry*, 17 (2013) 2035.
15. K.Y. Lee, H. Qian, H.T. Feng, J.J. Blaker, S.G. Kazarian and A. Bismarck, *Journal of Materials Science*, 48 (2013) 367.
16. Y.J. Ou, C. Peng, J.W. Lang, D.D. Zhu and X.B. Yan, *New Carbon Materials*, 77 (2014) 1196.
17. B. Kishore, D. Shanmughasundaram, T.R. Penki and N. Munichandraiah, *Journal of Applied Electrochemistry*, 44 (2014) 903.
18. M.Y. Zhang, X.J. Jin and Q. Zhao, *New Carbon Materials*, 29 (2014) 89.
19. C.S. Lim, K.H. Teoh, C.W. Liew and S. Ramesh, *Ionics*, 20 (2014) 251.
20. D. Tashima, H. Yoshitama, T. Sakoda, A. Okazaki and T. Kawaji, *Electrochimica Acta*, 77 (2012) 198.
21. K. Wang, Y. Cao, Z. Gu, P. Ahrenkiel, J. Lee and Q.H. Fan, *Rsc Advances*, 6 (2016) 26738.
22. M. Suleman, Y. Kumar and S.A. Hashmi, *Journal of Solid State Electrochemistry*, 19 (2015) 1347.
23. M. Zhang, X. Jin and Y. Wu, *Wood Research*, 58 (2013) 81.
24. N.I. Globa, O.B. Pushyk, D.G. Gromadskyi, O.I. Milovanova and S.A. Kirillov, *Russian Journal of Applied Chemistry*, 89 (2016) 1000.
25. S.H. Kwon, E. Lee, B.S. Kim, S.G. Kim, B.J. Lee, M.S. Kim and C.J. Ji, *Korean J. Chem. Eng.*, 32

(2015) 248.

26. X. Cai, R. Ren, M. Zhang, X. Jin and Q. Zhao, *Bioresources*, 10 (2015)
27. J.P. Tey, A.K. Arof, M.A. Yarmo and M.A. Careem, *Journal of New Materials for Electrochemical Systems*, 18 (2015) 183.
28. S. Ravulapalli and R. Kunta, *Journal of Fluorine Chemistry*, 193 (2017) 58.
29. T. Rime, M. Hartmann, B. Stierli, A.M. Anesio and B. Frey, *Soil Biology & Biochemistry*, 98 (2016) 30.
30. N. Muthuswamy, M.E.M. Buan, J.C. Walmsley and M. Rønning, *Catalysis Today*, (2017)
31. K.C. Bedin, A.C. Martins, A.L. Cazetta, O. Pezoti and V.C. Almeida, *Chem. Eng. J.*, 286 (2016) 476.
32. C.C. Huang and Y.Z. Chen, *Journal of the Taiwan Institute of Chemical Engineers*, 44 (2013) 611.
33. S. Guo, J. Peng, W. Li, K. Yang, L. Zhang, S. Zhang and H. Xia, *Appl. Surf. Sci.*, 255 (2009) 8443